

Figure 1. Far-infrared spectra of nickelocene in a krypton matrix at 4 K in various magnetic fields (B , in Tesla). Resolution was 0.5 cm^{-1} ; each trace was for 1000 scans.

The specific details of the experimental apparatus will be reported elsewhere. It consists of an Oxford SpectroMag SM4 containing a split-coil superconducting magnet capable of attaining 5 T with a homogeneity of 1 part in 10^4 over a 2 cm diameter, but with an appendage at the lower end to allow matrices to be made in the usual way.⁵ The sample was condensed on a gold-plated copper surface cooled to 4 K by a continuous flow of liquid helium. After the matrix was prepared, the gold surface was raised into the magnet, and infrared spectra were measured by reflection. IR spectra were measured with a vacuum Fourier transform spectrometer (Bruker IFS-113V) using 0.5 cm^{-1} resolution with detection in the far infrared by a liquid helium (pumped on to $\sim 1.6\text{ K}$) cooled silicon bolometer (Infrared Laboratories, Tucson, AZ). $\text{Ni}(\text{Cp})_2$, purchased from Strem Chemicals and purified by vacuum sublimation, was vaporized at $\sim 50\text{ }^\circ\text{C}$ and codeposited with argon or krypton gas. The rare gases were admitted at a rate of 10 mmol/h, and the matrix/nickelocene ratio was estimated to be 50–100. The deposition time was 2–3 h.

Figure 1 shows the absorption spectra of nickelocene trapped in a krypton matrix measured at zero and successively higher magnetic fields. Vibrational bands at higher frequencies agree well with those determined elsewhere⁶ and are unaffected by the magnetic field. The zero-field magnetic dipole transition occurs here at $32.4(2)\text{ cm}^{-1}$. A similar spectrum appears in argon at $32.5(2)\text{ cm}^{-1}$, but its half-width is about 1 cm^{-1} rather than the 0.5 cm^{-1} in Figure 1, perhaps due to a more concentrated matrix. [We also observed the absorption of pure solid nickelocene condensed on the gold surface at 4 K. The zero-field transition occurred at $34.2(2)\text{ cm}^{-1}$ with splitting and shifted to a lower frequency at 4 T. This value is in the direction expected from the χ values of Baltzer et al.,³ but not from the INS result.] It is significant that the values of $D = 32.5\text{ cm}^{-1}$ agree in the two matrices and presumably represent the value closest to that in the gas phase. The discrepancy of about 1 cm^{-1} from the value of Baltzer et al.,⁴ which was extrapolated to eliminate nickelocene intermolecular interactions, is then probably due to a remaining matrix effect, i.e., an environment of solid ruthenocene versus rare gas, causing a slightly increased magnetic anisotropy. From our past experience with variation of the zfs of small molecules with matrix gas,⁷ we would have expected a larger ΔD from the argon to krypton matrices, but apparently the sandwich molecule is more autonomous and inert to these relatively small perturbations.

In the ESR of randomly oriented molecules in a rigid medium, the spectra are dominated by the "perpendicular" lines, but near zero field these features are shifted much less than the "parallel" features by an increasing magnetic field. If only the lowest triplet Zeeman level is populated at 4 K, then for positive D :⁸

$$\Delta M_s = \pm 1 \quad \Delta v_{\parallel} = \pm g_{\parallel} \beta B / hc \cong \pm 0.93\text{ cm}^{-1} / \text{T}$$

$$\Delta v_{\perp 1} = (-D/2h) + [(D/h)^2 + 4(g_{\perp} \beta B / hc)^2]^{1/2} / 2 \\ \cong +0.03\text{ to }+0.1\text{ cm}^{-1} / \text{T}$$

$$\Delta M_s = \pm 2 \quad \Delta v_{\perp 2} = 2\Delta v_{\perp 1}$$

Hence, the perpendicular features are shifted slightly to higher frequencies with increasing magnetic field, while the parallel features spread out symmetrically and lead to the broadening and weakening of the zero-field line, as seen in Figure 1.

Nickelocene has served as an interesting test case for far-infrared magnetic resonance spectroscopy, which we plan to apply generally to molecules with $|D| > 10\text{ cm}^{-1}$ and $S \geq 1$.

Acknowledgment. This research was supported by the National Science Foundation (CHE-8814297, -8813549, and -9114387). Acknowledgement is also made to the donors of the Petroleum Research Fund, administered by the American Chemical Society, for partial support of this research. We also thank Matthew Ryan and Professor D. Richardson for aid in the preparation of pure nickelocene.

(8) Wasserman, E.; Snyder, L. C.; Yager, W. A. *J. Chem. Phys.* **1964**, *41*, 1763–72. Weltner, W., Jr. *Magnetic Atoms and Molecules*; Dover: Mineola, NY, 1989; Chapter III.

NOESY Studies on the $\text{Fe}^{\text{III}}\text{Co}^{\text{II}}$ Active Site of the Purple Acid Phosphatase Uteroferrin

Richard C. Holz and Lawrence Que, Jr.*

*Department of Chemistry, University of Minnesota
Minneapolis, Minnesota 55455*

Li-June Ming*

*Department of Chemistry and Institute for
Biomolecular Science, University of South Florida
Tampa, Florida 33620*

Received February 25, 1992

Nuclear magnetic resonance spectroscopy is a very valuable tool for probing enzyme active sites.¹ Its application to paramagnetic metalloproteins has been hampered by the unfavorable electronic relaxation times of paramagnetic centers, which often result in relatively broad isotropically shifted ^1H NMR signals (typically $>100\text{ Hz}$).² Consequently, the large line widths and short T_1 values of isotropically shifted signals in paramagnetic metalloproteins were thought to render 2D experiments impractical. Recently, NOESY spectra have been successfully recorded on paramagnetic metalloproteins which exhibit relatively sharp isotropically shifted signals ($<150\text{ Hz}$) and thus facilitated signal assignments.³ In our effort to gain further insight into the active

(1) (a) Wüthrich, K. *NMR of Proteins and Nucleic Acids*; John Wiley & Sons: New York, 1986. (b) Bertini, I.; Molinari, N.; Niccolai, N. *NMR and Biomolecular Structure*; VCH: New York, 1991.

(2) Bertini, I.; Luchinat, C. *NMR of Paramagnetic Molecules in Biological Systems*; Benjamin & Cummings: Menlo Park, CA, 1986.

(3) (a) Emerson, S. D.; La Mar, G. N. *Biochemistry* **1990**, *29*, 1545–1556. (b) Busse, S. C.; Moench, S. J.; Satterlee, J. D. *Biophys. J.* **1990**, *58*, 45–51. (c) Banci, L.; Bertini, I.; Paola, T.; Tein, M.; Kirk, T. K. *Proc. Natl. Acad. Sci. U.S.A.* **1991**, *88*, 6956–6960. (d) Banci, L.; Bertini, I.; Paola, T.; Ferrer, J. C.; Mauk, A. G. *Inorg. Chem.* **1991**, *30*, 4510–4516. (e) Banci, L.; Bertini, I.; Briganti, F.; Luchinat, C.; Scozzafava, A.; Oliver, M. V. *Inorg. Chem.* **1991**, *30*, 4517–4524. (f) Bertini, I.; Briganti, F.; Luchinat, C.; Messori, L.; Monnanni, R.; Scozzafava, A.; Vallini, G. *FEBS Lett.* **1991**, *289*, 253–256. (g) Capozzi, F.; Luchinat, C.; Piccioli, M.; Viezzoli, M. S. *Eur. J. Biochem.* **1991**, *197*, 691–697. (h) Satterlee, J. D.; Erman, J. E. *Biochemistry* **1991**, *30*, 4398–4405. (i) Skjeldal, L.; Westler, W. M.; Oh, B.-H.; Krezel, A. M.; Holden, H. M.; Jacobson, B. L.; Rayment, I.; Markley, J. L. *Biochemistry* **1991**, *30*, 7363–7368. (j) Satterlee, J. D.; Russell, D. J.; Erman, J. E. *Biochemistry* **1991**, *30*, 9072–9077. (k) Banci, L.; Bertini, I.; Paola, T.; Oliver, M. V. *Eur. J. Biochem.* **1992**, *204*, 107–112.

(5) Van Zee, R. J.; Ferrante, R. F.; Zeringue, K. J.; Weltner, W., Jr. *J. Chem. Phys.* **1988**, *88*, 3465–74.

(6) See, for example: Chlor, K.; Lucazeau, G.; Sourisseau, C. *J. Raman Spectrosc.* **1981**, *11*, 183–198 and references given therein.

(7) Smith, G. R.; Weltner, W., Jr. *J. Chem. Phys.* **1975**, *62*, 4592–4604.

Table I. ^1H NMR (360 MHz) Parameters for $\text{Fe}^{\text{III}}\text{Co}^{\text{II}}\text{Uf}$ at 40 °C in H_2O

signal	chemical shift (ppm)	line width ^a (fwhm ^b Hz)	T_1 (ms) ^c	integration ^d
A ^e	99	1090 ^f		2
B	83	950	48	1
C	68	970	21	2
D	64	980	26	1
E	54	1670	18	4
F	30.5	690	31	1
G	28.5	470	46	1
H	22.4	940	23	2
I	17.7	230 ^g	80 ^g	1
I'	17.3	230 ^g	80 ^g	2
J	10.8	100 ^f		2

^aThe line widths of signals C, D, F, and G were obtained by deconvolution using a Lorentzian fitting routine. ^bFull width at half maximum. ^c T_1 values were obtained at 300 MHz and 40 °C following the methods outlined in ref 6. ^dRelative areas based on the area of signals F and G.⁶ ^eSolvent exchangeable. ^fValues obtained at 300 MHz and 40 °C. ^gLine width and T_1 values are a total of the overlapped signals at 17.3 ppm, which includes signals I and I'.

site of uteroferrin (Uf), we have obtained phase-sensitive NOESY spectra of $\text{Fe}^{\text{III}}\text{Co}^{\text{II}}\text{Uf}$ in which clear NOE connectivity is observed between isotropically shifted signals with kilohertz line widths at 360 MHz. From these data, several of the active site ligands were identified.

Uteroferrin, the 35 kDa purple acid phosphatase from porcine uterus,⁴ exhibits well-resolved isotropically shifted ^1H NMR resonances arising from an $\text{Fe}^{\text{III}}\text{Fe}^{\text{II}}$ dinuclear active site.^{5,6} Replacement of Fe^{II} with Co^{II} (which typically has shorter electronic T_1 values)² affords a catalytically active species⁷ which exhibits many additional isotropically shifted signals in the +100 to 10 ppm range (Figure 1, Table I) with relaxation times (T_1) 2–4 times longer than those of the native enzyme. Among these resonances, signal A at 99 ppm (not shown) is solvent exchangeable and consequently is assigned to the imidazole NH protons of coordinated histidine residues. This signal is somewhat asymmetric and integrates to two protons. The sharper component is assigned to a histidine ligand at the high-spin Co^{II} center, while the broader feature is assigned to a histidine ligand at the high-spin Fe^{III} center. Since the T_1 values for the resonances in the 90 to 10 ppm region ranged from 18 to 80 ms (Table I), a NOESY experiment was attempted despite the broadness of the isotropically shifted resonances. A phase-sensitive (TPPI) NOESY spectrum of $\text{Fe}^{\text{III}}\text{Co}^{\text{II}}\text{Uf}$ was recorded at 40 °C which clearly showed NOE connectivity between many of the isotropically shifted signals (Figure 1). The correlation information obtained was verified by 1D NOE experiments and has facilitated the assignment of many of the isotropically shifted signals in conjunction with chemical shift and T_1 information.

Signals B, C, E, and J are all associated with the tyrosine bound to the Fe^{III} center. The signals at 81 (B) and 10.8 (J) ppm correspond to the $\beta\text{-CH}_2$ protons of tyrosine on the basis of their strong cross-relaxation and similarities in their chemical shifts with those of native Uf (86.6 and 15.1 ppm at 31 °C).^{5,6} 1D NOE studies indicate that signal B is also weakly correlated to signals C (68 ppm) and E (54 ppm), which correspond to the tyrosine

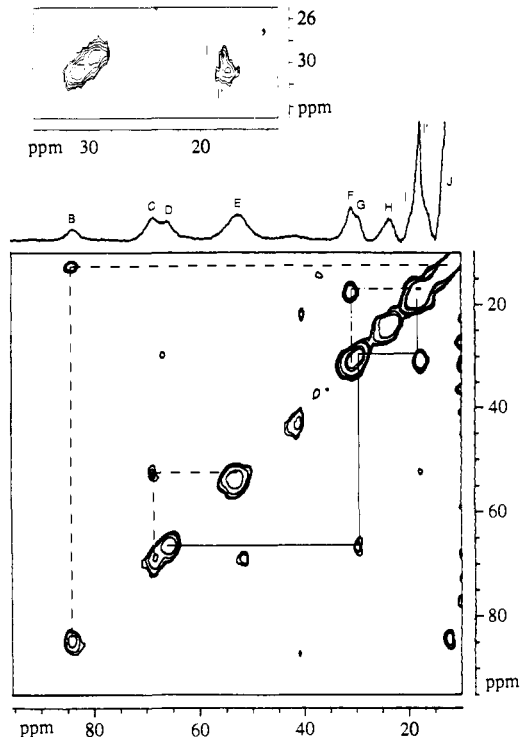


Figure 1. Phase-sensitive (TPPI) ^1H NOESY spectrum obtained at 360 MHz (Bruker AMX-360) on a 2.5 mM sample of $\text{Fe}^{\text{III}}\text{Co}^{\text{II}}\text{Uf}$ in a buffered D_2O solution (100 mM acetate, 200 mM NaCl, pH 5.3) at 40 °C. This spectrum was obtained with a 15-ms mixing time and 512 data points in the F_1 dimension (which gave a digital resolution of 180 Hz) and 1024 data points in the F_2 dimension. A 5% shifted Gaussian weighting function was applied prior to Fourier transformation followed by base line correction in both dimensions. Inset: Expanded view of the cross signals at ~ 17 ppm along the F_2 dimension. Two overlapped signals can be clearly resolved with chemical shifts of 17.7 (I) and 17.3 (I') ppm by applying a 30% shifted Gaussian.

2,6-protons; the latter two signals are correlated to each other because of chemical exchange (i.e., rotation of the phenolate ring with respect to the $\text{C}_\beta\text{-C}_\gamma$ bond). Furthermore, clear NOE cross signals are observed between signals F (30.5 ppm) and I' (17.3 ppm) (Figure 1 inset). These protons are correlated with the exchangeable signal A from 1D NOE studies and are therefore associated with histidine residues coordinated at the dinuclear active site.

The NOESY spectrum also shows remarkably clear cross-relaxation between signals D (64 ppm) and G (28.5 ppm) (Figure 1) and between signals G and I (17.7 ppm) (Figure 1 inset), suggestive of an ABX spin system. Such a pattern can be assigned to a $\text{YCH}_2\text{CH} < \text{amino acid side chain with Y ligated to the metal center}$. Of the possible amino acid residues which could produce such an ABX spin pattern, only aspartate or glutamate can give rise to the observed isotropic shifts and T_1 ($\propto r_{\text{Fe-H}}^6$) values.^{6,9} Indeed, the chemical shifts and T_1 values for signals D, G, and I are consistent with those assigned to the aspartate residue bound to the Co^{II} center of CuCoSOD .¹⁰ Therefore, signals D, G, and I are assigned to an aspartate or glutamate residue coordinated to the Co^{II} center of $\text{Fe}^{\text{III}}\text{Co}^{\text{II}}\text{Uf}$. This assignment is consistent with recent EXAFS studies on native Uf¹¹ and provides the first definitive evidence of a coordinated carboxylate.^{6,12}

(4) Chen, T. T.; Bazer, F. W.; Cetorelli, J. J.; Pollard, W. E.; Roberts, R. M. *J. Biol. Chem.* **1973**, *248*, 8560–8566.

(5) Lauffer, R. B.; Antanaitis, B. C.; Aisen, P.; Que, L., Jr. *J. Biol. Chem.* **1983**, *258*, 14212–14218.

(6) Scarrow, R. C.; Pyrz, J. W.; Que, L., Jr. *J. Am. Chem. Soc.* **1990**, *112*, 657–665.

(7) The preparation of $\text{Fe}^{\text{III}}\text{Co}^{\text{II}}\text{Uf}$ was achieved by a modification of the method reported by Beck et al.⁸ Removal of a single iron atom from reduced Uf followed by the subsequent addition of 1 equiv of Co^{II} under anaerobic conditions produced the desired mixed-metal enzyme. After 3 days at ambient temperature a pink enzyme solution was recovered ($\lambda_{\text{max}} = 510$ nm, $\epsilon = 4000$ $\text{M}^{-1}\text{cm}^{-1}$) which exhibited $\sim 50\%$ of the original activity, was EPR silent, and by atomic absorption spectroscopy analysis contained a single mole of iron and cobalt per mole of protein.

(8) Beck, J. L.; Keough, D. T.; de Jersey, J.; Zerner, B. *Biochim. Biophys. Acta* **1984**, *791*, 357–363.

(9) The $r_{\text{M-H}}$ value estimated for D and G is 5 ± 0.5 Å,⁶ which is too long for $\beta\text{-CH}_2$ protons of Cys and Ser and too short for Tyr. Though the T_1 values are appropriate for N_2 -coordinated His, $\beta\text{-CH}_2$ protons of such residues exhibit much smaller isotropic shifts.^{6,10}

(10) Banci, L.; Bencini, A.; Bertini, I.; Luchinat, C.; Piccioli, M. *Inorg. Chem.* **1990**, *29*, 4867–4873.

(11) True, A. E.; Scarrow, R. C.; Holz, R. C.; Que, L., Jr. *J. Am. Chem. Soc.*, submitted for publication.

(12) Vincent, J. B.; Olivier-Lilley, G. L.; Averill, B. A. *Chem. Rev.* **1990**, *90*, 1447–1467.

In conclusion, we report the first NOESY spectrum of a paramagnetic metalloprotein which exhibits line widths at half-height greater than 1000 Hz at 360 MHz. Moreover, these studies have facilitated the assignment of several of the observed isotropically shifted signals. These data also establish for the first time that a carboxylate moiety resides at the active site of Uf. Our studies suggest that NOESY spectra can be obtained for isotropically shifted proton signals which are comparatively broad, provided that the T_1 values are sufficiently long to allow NOE buildup to occur. We estimate T_1 values greater than 10 ms to provide ample time to observe NOE buildup for systems of this type.

Acknowledgment. This work was supported by a grant from the National Science Foundation (Grant No. DMB-9104669, L.Q.). R.C.H. is grateful for an NIH postdoctoral fellowship (GM-13919). L.-J.M. is grateful for a startup grant from the University of South Florida (USF). The Bruker AMX-360 NMR spectrometer was purchased with funds provided by the National Science Foundation and USF.

Additions of Malononitrile Radicals to Alkenes: New Examples of 1,2-Asymmetric Induction in Iodine and Phenylselenium Transfer Reactions

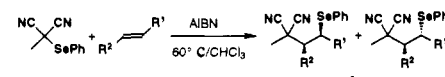
Dennis P. Curran* and Gebhard Thoma

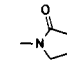
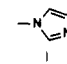
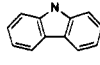
Department of Chemistry
University of Pittsburgh
Pittsburgh, Pennsylvania 15260

Received January 31, 1992
Revised Manuscript Received April 13, 1992

One of the current frontiers in radical chemistry is the control of acyclic stereochemistry,¹ and recent work has focused on 1,2-asymmetric induction.²⁻⁴ We have introduced iodomalnonitriles as useful reagents for radical addition and annulation reactions (eq 1, X = I),⁵ and we felt that these or related reagents would be especially useful for study of 1,2-asymmetric induction in radical reactions.^{4b} In attempting to study asymmetric reactions of heteroatom-substituted radicals, we learned that iodomalnonitriles do not add cleanly to oxygen-, sulfur-, or nitrogen-substituted alkenes ($R^1 = \text{OR}, \text{SR}, \text{NR}_2$).⁶ To solve this problem, we introduce a new class of reagents, (phenylseleno)malononitriles (X = SePh),^{7,8} and describe the first examples of asymmetric selenium

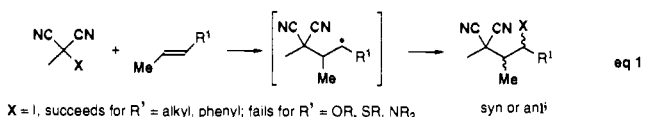
Table I. Additions of **1** to Alkenes



Alkene 2	R ¹	R ²	Time	Yield ^a	syn/anti (or cis/trans)
a	C ₆ H ₉	H	40 h	97%	-
b	C ₆ H ₅	H	120 h	84%	-
c	OC ₂ H ₅	H	2 h	96%	-
d	OCOCH ₃	H	24 h	97%	-
e	SC ₆ H ₅	H	2 h	97%	-
f		H	5 h	91%	-
g		H	120 h ^b	84%	-
h		H	16 h	97%	-
i	-CH ₂ CH ₂ CH ₂ -		120 h	55%	(0/100)
j	-OCH ₂ CH ₂ CH ₂ -		120 h	78%	(30/70)
k	C ₆ H ₅	CH ₃	240 h	80%	80/20
l	OC ₂ H ₅	CH ₃ ^c	70 h	92%	25/75
m	SC ₆ H ₅	CH ₃ ^c	40 h	73%	10/90
n	See entry h	CH ₃	120 h	70%	90/10

^a Procedure: A CHCl₃ solution of **1** (0.1 M), the alkene (2–3 equiv), and AIBN (5%) was heated at 60 °C. For slow reactions, additional AIBN (5%) was added once per day. After **1** was consumed, the solvent was evaporated and the product was purified by chromatography on silica gel (ether/hexanes, 1/10). ^b Ten equivalents of alkene used. ^c E/Z mixture.

transfer reactions of benzylic ($R^1 = \text{Ph}$), oxygen-substituted ($R^1 = \text{OR}$), sulfur-substituted ($R^1 = \text{SPh}$), and nitrogen-substituted ($R^1 = \text{NR}_2$) radicals. Perhaps most importantly, additions of iodomalnonitriles to disubstituted alkenes provide the first examples of high 1,2-asymmetric induction in reactions of alkyl radicals bearing no conjugating substituents (X = I, $R^1 = \text{alkyl}$).



X = I, succeeds for $R^1 = \text{alkyl}, \text{phenyl}$; fails for $R^1 = \text{OR}, \text{SR}, \text{NR}_2$
X = SePh, succeeds for $R^1 = \text{phenyl}, \text{OR}, \text{SR}, \text{NR}_2$; fails for $R^1 = \text{alkyl}$

Methyl(phenylseleno)malononitrile (**1**) is readily available by the reaction of the anion of methylmalononitrile with benzene-selenenyl bromide. In a typical addition reaction (Table I, entry a), selenomalnonitrile **1**, 1-hexene, and AIBN were heated in CHCl₃ at 60 °C. After 40 h, the reaction was complete, and we isolated adduct **3a** in 97% yield. Reactions of **1** with other monosubstituted alkenes are summarized in Table I, entries a–h. Additions occur not only with alkyl- and phenyl-substituted alkenes (which form adducts with iodomalnonitriles⁴) but also with *O*-alkyl-, *O*-acyl-, *S*-phenyl, *N*-heterocycle-, and *N*-acyl-substituted alkenes (which do not form adducts with iodomalnonitriles). These reactions do not occur in the absence of AIBN, and we believe that a standard radical chain mechanism is involved. The malononitrile radical adds to the alkene, and the adduct radical abstracts a phenylselenium group^{7,8} from the (phenylseleno)malononitrile to give the product **3a** and the starting radical.

Entries i–n in Table I summarize the additions of **1** to representative 1,2-disubstituted alkenes. Although reaction times can be very long (3–10 days), yields are consistently high. Product ratios do not change over time, so we believe that the observed ratios are kinetically controlled. Regioselectivities are very high

(8) Byers and co-workers recently reported examples of phenylselenium-transfer addition and cyclizations of selenomalonic esters. (a) Byers, J. H.; Gleason, T. G.; Knight, K. S. *J. Chem. Soc., Chem. Commun.* 1991, 354. (b) Byers, J. H.; Lane, C. G. *Tetrahedron Lett.* 1990, 31, 5697. (c) See also: Kropp, P. J.; Fryxell, G. E.; Tubergen, M. W.; Hager, M. W.; Harris, G. D., Jr.; McDermott, T. P., Jr.; Tornero-Velez, R. *J. Am. Chem. Soc.* 1991, 113, 7300.

(1) Review: Porter, N. A.; Giese, B.; Curran, D. P. *Acc. Chem. Res.* 1991, 24, 296.

(2) Recent leading references to carbonyl-substituted radicals: (a) Hart, D. J.; Huang, H. C.; Krishnamurthy, R.; Schwartz, T. *J. Am. Chem. Soc.* 1989, 111, 7507. (b) Guindon, Y.; Lavallee, J. F.; Llinas-Brunet, M.; Horner, G.; Rancourt, J. *J. Am. Chem. Soc.* 1991, 113, 9701. (c) Bulliard, M.; Zehnder, M.; Giese, B. *Helv. Chim. Acta* 1991, 74, 1600. (d) Hart, D. J.; Krishnamurthy, R. *Synlett* 1991, 412. (e) Curran, D. P.; Abraham, A. C.; Liu, H. *J. Org. Chem.* 1991, 56, 4335. (f) Beckwith, A. L. J.; Hersperger, R.; White, J. M. *J. Chem. Soc., Chem. Commun.* 1991, 1151. (g) Snider, B. B.; Wan, B. Y.-F.; Buckmann, B. O.; Foxmann, B. M. *J. Org. Chem.* 1991, 56, 328. (h) Phosphine oxide-substituted radicals: Brandi, A.; Cicchi, S.; Goti, A.; Pietrusiewicz, K. M. *Tetrahedron Lett.* 1991, 32, 3265.

(3) Oxygen-substituted radicals: Giese, B.; Damm, W.; Dickhaut, J.; Wetterich, F.; Sun, S.; Curran, D. P. *Tetrahedron Lett.* 1991, 32, 6097.

(4) Benzylic radicals: (a) Giese, B.; Bulliard, M.; Zeitz, H.-G. *Synlett* 1991, 425. (b) Curran, D. P.; Thoma, G. *Tetrahedron Lett.* 1991, 32, 6307.

(5) (a) Curran, D. P.; Seong, C.-M. *J. Am. Chem. Soc.* 1990, 112, 9401. (b) Curran, D. P.; Seong, C. M. *Tetrahedron* 1992, 48, 2157, 2175.

(6) Iodomalonic esters did not add to such alkenes either. Curran, D. P.; Chen, M.-H.; Spletzer, E.; Seong, C. M.; Chang, C.-T. *J. Am. Chem. Soc.* 1989, 111, 8872.

(7) Selenium-transfer additions of Se-heteroatom bonds are well known. Examples and leading references: (a) Back, T. G.; Krishna, M. J. *J. Org. Chem.* 1988, 53, 2533. (b) Back, T. G.; Krishna, M. V.; Muralidharan, K. R. *Tetrahedron Lett.* 1987, 28, 1737. (c) Toru, T.; Seko, T.; Maekawa, E.; Ueno, Y. *J. Chem. Soc., Perkin Trans. 1* 1989, 1927. (d) Ogawa, A.; Yokoyama, H.; Yokoyama, K.; Masawaki, T.; Kambe, N.; Sonoda, N. *J. Org. Chem.* 1991, 56, 5721.